Very Efficient Generation of Quinone Methides through Excited State Intramolecular Proton Transfer to a Carbon Atom

ARTICLE *in* CHEMISTRY - A EUROPEAN JOURNAL · AUGUST 2012

Impact Factor: 5.73 · DOI: 10.1002/chem.201201144 · Source: PubMed

6 AUTHORS, INCLUDING:

Jakov Ivkovic
Graz University of Technology
5 PUBLICATIONS **61** CITATIONS
SEE PROFILE

Lily Wang
University of Victoria
11 PUBLICATIONS **57** CITATIONS
SEE PROFILE

Momir Mališ
Ruđer Bošković Institute
12 PUBLICATIONS **99** CITATIONS
SEE PROFILE

CHEMISTRY
A EUROPEAN JOURNAL

FULL PAPER

DOI: 10.1002/chem.201201144

Very Efficient Generation of Quinone Methides through Excited State Intramolecular Proton Transfer to a Carbon Atom

Nikola Basarić,*[a] Nađa Došlić,*[b] Jakov Ivković,[a] Yu-Hsuan Wang,[c] Momir Mališ,[b] and Peter Wan*[c]

Abstract: Irradiation of 2-phenyl-1-naphthol (**6**) in CH_3CN/D_2O (3:1) leads to very efficient incorporation of deuterium at the *ortho*-positions of the adjacent phenyl ring (overall $\Phi = 0.73 \pm 0.07$), along with minor incorporation at the naphthalene positions 5 and 8. These finding are explained by excited state intramolecular proton transfer (ESIPT) from the phenolic OH group to the corresponding carbon atoms, the main pathway giving rise to quinone methide (QM) **7**, which has been characterized by LFP ($\tau \approx 20$ ns; 460 nm). The ESIPT reaction paths have been explored with the second order approximate coupled cluster (CC2) method. In nonprotic solvents the ESIPT from the naphthol O-H to the *ortho*-position of the phenyl ring proceeds in a barrierless manner along the ^1L_a energy surface via a conical intersection with the S_0 state, delivering **7**. In aqueous solvent, clusters with H_2O are formed wherein proton transfer (PT) to solvent and a H_2O-mediated relay mechanism gives rise to naphtholates and QMs. The results are compared with 2-phenylphenol (**3**) that also undergoes barrierless ESIPT giving a QM via a conical intersection. However, due to an unfavorable conformation in the ground state, the quantum efficiency for ESIPT of **3** is significantly lower (Φ for D-exchange = 0.041). These results show that ESIPT from phenol to carbon need not be an intrinsically inefficient process.

Keywords: ab initio calculations · deuterium exchange · naphthols · photochemistry · quinone methides

Introduction

Excited state intramolecular proton transfer (ESIPT) has been the focus of intensive research in the last four decades because of its fundamental interest,[1] as well as many applications,[2] including sensing,[3] photolabeling,[4] laser dyes,[5] photostabilizers,[6] scintillators,[7] photoswithing in fluorescent proteins,[8] long-lived pH jumps,[9] or switching of polymorphs.[10] According to Kasha, ESIPT can be divided into several mechanistic scenarios including intrinsic intramolecular proton transfer (the true ESIPT), concerted biprotonic transfer, proton-relay tautomerization, and catalysis of proton transfer.[11] The most common acidic group in the ESIPT reactions is the phenolic OH or amine NH, whereas the basic site is usually a heteroatom such as pyridine nitrogen or carbonyl oxygen.[1] Although some examples are known wherein protonation of a carbon can compete with the protonation of heteroatoms,[12] ESIPT to carbon usually takes place with much lower quantum efficiency.[13–19] Consequently, it is often overlooked as a possible nonradiative relaxation pathway in biological molecules,[20] or as a viable synthetic route to quinone methides (QM).[21] The later are important reactive intermediates in organic synthesis[22] capable of cross-linking DNA,[23] and involved in the antineoplastic action of some antibiotics.[24]

To date, several examples of ESIPT to carbon atoms of the aromatic ring have been described.[12–20] One prominent example is that of 1-naphthol (**1**). In S_1, **1** becomes significantly more acidic ($pK^*_a = 0.4$),[13] and in addition to proton transfer (PT) to solvent, a solvent-assisted transfer of the OH proton to the carbon atom at position 5 of the ring takes place giving quinone methide (QM) **2** with a quantum efficiency of 0.11 (Reaction (1)).[13,14] In addition, as a general reaction, ESIPT from the phenol OH to the carbon atoms of the adjacent phenyl,[15] naphthyl,[14,16] anthryl,[17] terphenyl,[18] or pyrenyl ring[19] have been reported. ESIPT in 2-phenylphenol (**3**) gives QM **4**, whereas solvent-assisted ESPT gives rise to QM **5** (Reaction (2)). Formation of QMs **4** and **5** was inferred due to regiospecific incorporation of deuteri-

[a] Dr. N. Basarić, J. Ivković
Department of Organic Chemistry and Biochemistry
Ruđer Bošković Institute
Bijenička cesta 54, 10000 Zagreb, (Croatia)
Fax: (+)385 (1) 4680-195
E-mail: nbasaric@irb.hr

[b] Dr. N. Došlić, M. Mališ
Department of Physical Chemistry
Ruđer Bošković Institute
Bijenička cesta 54, 10000 Zagreb, (Croatia)
Fax: (+)385 (1) 4680-245
E-mail: nadja.doslic@irb.hr

[c] Dr. Y.-H. Wang, Dr. P. Wan
Department of Chemistry
University of Victoria
Box 3065, Victoria BC, V8W 3V6, (Canada)
Fax: (+)1 (250) 721-7147
E-mail: pwan@uvic.ca

Supporting information for this article is available on the WWW under http://dx.doi.org/10.1002/chem.201201144.

um on irradiation in D_2O (D-exchange $\Phi = 0.041$).[15] However, QMs **4** and **5** from these ESIPT reactions have never been detected spectroscopically. In addition, the efficiency of the QM formation by ESIPT or ESPT to carbon in all examples known to date is low.

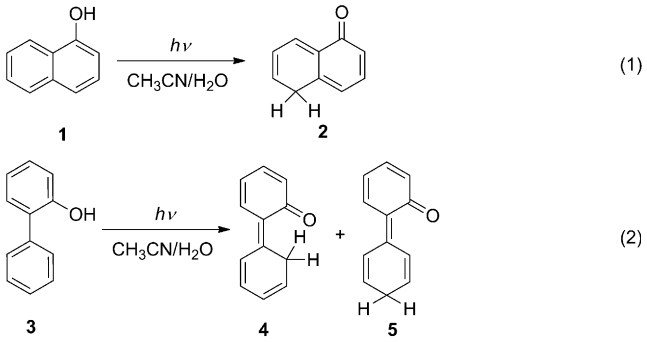

(1)

(2)

Our combined experimental and theoretical study describes very efficient ESIPT in 2-phenyl-1-naphthol (**6**) where the *ortho*-carbon atom of the adjacent phenyl ring is the basic site. The process has been investigated by irradiations in the presence of D_2O, wherein regiospecific incorporation of deuterium denotes the ESIPT pathway. We show that ESIPT operates via a conical intersection with the ground state which is the dominant de-excitation pathway from the singlet excited state surface in nonprotic solvent. In aqueous media, PT to solvent delivers naphtholate and a relay mechanism gives rise to QMs. By demonstrating that protonation of an adjacent carbon atom takes place more efficiently than PT to H_2O bulk, our results additionally support the finding that the intrinsic rate constant for the protonation of carbon is not necessarily lower than for the protonation of heteroatoms.[25] Furthermore, this work demonstrate that QMs can be delivered in high yields through an efficient photochemical reaction - ESIPT to carbon atom.

Results and Discussion

Naphthol **6** was prepared from 1-naphthol (**1**) and pentaphenyl bismuth according to an already described procedure.[26] 1-Methoxy-2-phenylnaphthalene (**6OMe**)[27] was obtained from **6** by methylation using CH_3I under basic conditions (K_2CO_3) in a nonprotic solvent.

To probe for the ESIPT pathway involving carbon atoms as the basic site, irradiations of **1** were performed in CH_3CN/D_2O (3:1). After aqueous work-up the samples were analyzed by MS and NMR to determine the extent and position of deuteration. After 1 h photolysis of **6** in CH_3CN/D_2O ($c(D_2O) = 0.3$ M) we observed almost complete exchange of the H-atoms by deuterium at the *ortho*-position of the adjacent phenyl ring (see ^{1}H NMR in the Supporting Information) indicating formation of **6-D** and **6-2D** (reaction (3)). Mass spectra were in accordance with the NMR, indicating presence of mostly dideuterated species. On photolysis in CH_3CN/D_2O (3:1, $c(D_2O) = 14$ M) under the same conditions, in addition to the formation of **6-D** and **6-2D**, ^{1}H NMR spectrum showed incorporation of deuterium at the naphthalene position 5 (51%), 8 (37%), and 4, 6, or 7 (30%), whereas MS indicated the presence of 30% dideuterated, 36% trideuterated, and 18% of tetradeuterated species. Parallel irradiations of the samples with different D_2O concentration taken to lower conversions indicated that D-exchange is up to 10–20% more efficient at lower D_2O content and primarily takes place at the adjacent phenyl ring. Irradiation of the corresponding methoxy derivative, **6OMe** under the identical conditions gave no D-exchange, indicating that the phenolic OH is essential for the D-exchange. These findings are in agreement with operation of ESIPT and solvent-assisted PT, delivering QMs (see below) that on subsequent tautomerization give rise to deuterated compounds. The alternative mechanism which involves protonation of the naphthol by H_2O (D_2O) and formation of carbocations, as demonstrated by Shizuka and Tobita for methoxynaphthalenes,[28] at pH 7 probably does not take place or takes place with significantly lower quantum efficiency.

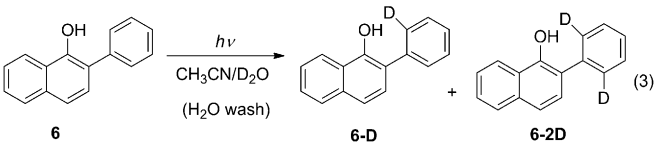

(3)

Quantum yield of D-incorporation was determined by use of a secondary actinometer, D-exchange in 2-phenylphenol (**2**, $\Phi = 0.041$),[15] and a primary one (photolysis of valerophenone to give acetophenone $\Phi = 0.65$).[29] Both standards gave similar values for the D-exchange Φ, with the mean value 0.73 ± 0.07. Taking into account the expected isotope effect (assuming the similar values as in the thermal reversal noncatalyzed enolization giving phenols and naphthols $k_{H2O}/k_{D2O} = 1.5$),[30] such a high Φ for the exchange suggests that approximately 90% of the molecules deactivate from the S_1 giving the corresponding QMs **7**, and some smaller amounts of QM **8** and zwitterion **9**, as shown in Scheme 1.[31] To the best of our knowledge this is the most efficient ESIPT to carbon ever reported.

The absorption spectrum of **6** is characterized by a broad low-energy band between 275 and 350 nm, typical for α-naphthols due to overlapped L_a and L_b transitions. However, fluorescence spectra of **6** in aprotic solvents are narrower than those of α-naphthols (half band with 3773 cm^{-1}), more similar to β-naphthols. In cyclohexane or CH_3CN, fluorescence of **6** is weak, with fluorescence quantum yields of $\Phi_f = 0.0108 \pm 0.0002$, and $\Phi_f = 0.031 \pm 0.001$, respectively. Fluorescence decays in CH_3CN and cyclohexane can be best fitted to a three-exponential function, suggesting presence of three fluorescent excited states. In CH_3CN the measured decay times are: 0.3 ± 0.1 (30%), 1.7 ± 0.1 (20%), and 10.3 ± 0.3 ns

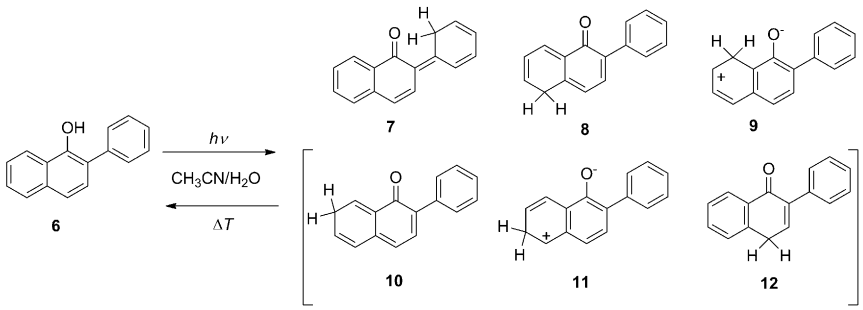

Scheme 1.

(50%). The low Φ_f and short average τ_f is in accordance with the efficient ESIPT deactivation pathway from S_1 giving QM **7**. On addition of H_2O to the CH_3CN solution, fluorescence increases, that is, H_2O lowers Φ of ESIPT. However, at high concentrations of H_2O, an additional shoulder appears at longer wavelength (475 nm) in the fluorescence spectrum corresponding to the naphtholate formed from **6** by an adiabatic PT to the solvent. The PT to the solvent with concomitant protonation of the distal carbon sites ultimately leads to the formation of QMs **8** and **9**, however with quantum yields that are lower by an order of magnitude.

Laser flash photolysis (LFP) was performed to probe for QMs that are formed by ESIPT or solvent-assisted PT (Figure 1 and Figures S14–S20 in the Supporting Information). In CH_3CN, LFP of **6** showed the presence of a short-lived transient absorbing at 350–570 nm (3.54–2.18 eV) with a lifetime of ≈20 ns. The transient was not affected by O_2 in accordance with its formation from the singlet excited state. In CH_3CN/D_2O (3:1) the decay kinetics of the transient was slower ($\tau \approx 60$–70 ns) than in CH_3CN-H_2O ($\tau \approx 35$–50 ns). The slower decay kinetics in the presence of D_2O is in agreement with slower H(D)-transfer due to the expected deuterium isotope effect.[30] LFP of **6OMe** that cannot undergo ESIPT did not give rise to the observed short-lived transient. Consequently, we assign the observed transient to QM **7**. The assignation is additionally corroborated by the calculated excitation energies of the QM **7**-H_2O clusters estimated in the range between 3.0–3.2 eV (see Figure 3). To the best of our knowledge, this is the first reported optical detection of a transient spectrum of a QM formed by ESIPT to an aromatic carbon atom. The transient spectra taken at longer times after the laser pulse (see Figure S16 in the Supporting Information) reveal absorptions with a maximum at 350 nm, and at 400–600 nm ($k = 1\times10^5 - 8\times10^4\ s^{-1}$, $\tau = 5$–12 μs). According to the comparison with the published spectra of naphthoxyl and phenoxyl radicals, the observed more persistent transient at 400–600 nm probably corresponds to minor formation of phenoxyl radicals by two-photon ionization giving radical cations and solvent electron, and subsequent deprotonation of radical cations.[32]

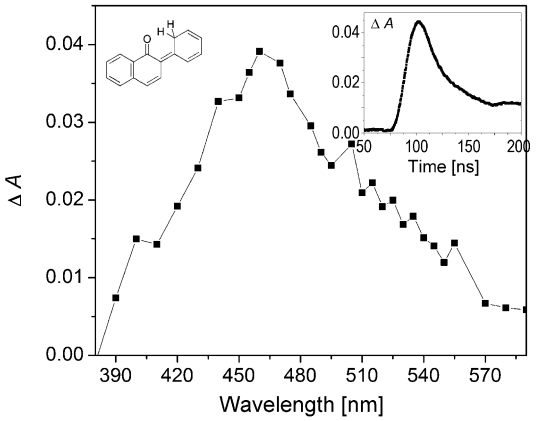

Figure 1. Transient absorption spectrum of **1** in O_2-purged CH_3CN solution 60 ns after the laser flash (inset: decay at 480 nm).

Ab initio calculations were employed to gain a deeper understanding of the efficient ESIPT in **6**. With respect to the rotation about the C–O bond (and orientation of the OH- and the adjacent phenyl), we distinguish between the *syn*-(**S**) and the *anti*-(**A**) conformations. Under experimental conditions for D-exchange, ($c(D_2O) = 0.3$ M), the number of D_2O molecules exceeded the number of reactant molecules by two orders of magnitude. Therefore, it is plausible to assume that clusters with H_2O are ubiquitously formed in solution. The minimum energy structures of **6** and the corresponding H_2O-cluster are *syn*-(**S6** and **S6·W**). The *anti*-conformations **A6** and **A6·W** are found 3.79 (2.63) and 3.94 (3.06) kcal mol^{-1} higher in energy in the gas phase (polarizable continuum, see Table S1 in the Supporting Information).

The RI-CC2 calculations of **S6** yield two energetically close π–π* transitions at 290 nm (S_1) and 273 nm (S_2) with comparable oscillator strengths (Table 1). In the first state, characterized as ^1L_a according to E. Pines,[33] the transition dipole is approximately directed along the long naphthalene axis. In the second state, ^1L_b, the dipole points along the short axis. Due to the phenyl interaction with the naphthol ring both transitions have charge transfer character. The leading excitations contributing to ^1L_a are shown in Figure 2 (insets, left). At its optimized geometry the ^1L_a state lies almost $\Delta E \approx 0.74$ eV below the vertical excitation. This is a consequence of substantial geometrical changes that the system experiences which include a 20 degree rotation of the phenyl ring. Specifically, the tilt of 57.1° between the two rings at S_0 minimum energy geometry is reduced to 36.0 at the ^1L_a optimized geometry leading to an effective shortening of the proton transfer distance from 2.38 on the S_0 to 1.99 Å on ^1L_a. Figure S4 and the graphical abstract display the difference in the electron densities between ^1L_a and the ground state. The transfer of negative charge from the naph-

Table 1. Vertical and adiabatic excitation energies of the lowest two excited singlet states of **S6**, **S6·W**, and **A6·W** computed using the RI-CC2/cc-pVDZ method and the components of the transition strength, f_x and f_y, directed approximately along the naphthalene long and short axes, respectively.[a]

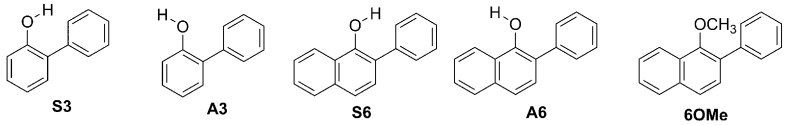

State	S6			S6·W			A6·W		
	ΔE [nm]	f_x	f_y	ΔE [nm]	f_x	f_y	ΔE [nm]	f_x	f_y
$^1\pi\,\pi^*$ (^1L_a)	290 (325)[a]	0.44	0.01	292 (356)[a]	0.53	0.13	293 (342)[a]	0.30	0.003
$^1\pi\,\pi^*$ (^1L_b)	273	0.10	0.50	275	0.001	0.58	281	0.18	0.68

[a] The value in parenthesis corresponds to adiabatic excitation energy.

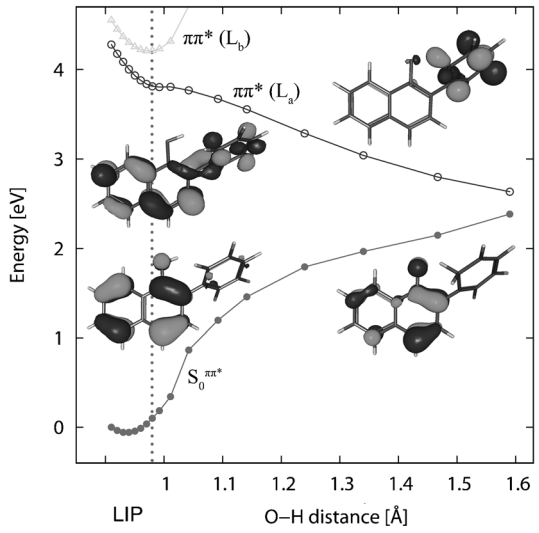

Figure 2. Linearly interpolated path (LIP) and relaxed scan of the **S6** ^1L_a state along the OH stretching coordinate. Insets: occupied (bottom) and unoccupied (top) molecular orbitals of the ^1L_a state at the vertical geometry (left) and at $R_{OH}=1.59$ Å (right).

thol oxygen (blue) to the phenyl *ortho*-carbon atom (red) and to the bond connecting the two subunits is apparent. Clearly, the charge redistribution sets the stage for the subsequent ESIPT.

Stretching of the O–H bond in the ^1L_a state of **6** promotes ESIPT to the phenyl ring, delivering QM **7**. The potential energy profiles for the ESIPT reaction path along the O–H···π bond is shown in Figure 2. A negligible barrier of <0.05 eV was found along this path. The elongation of the O–H bond and the increase of the torsional angle from 36.0 to 45.8 degrees, disrupt the conjugation of the naphthol π-electron system and leads to the strong destabilization of the ground state. The conical intersection (CI) of the ^1L_a and the ground electronic state is encountered $\approx$2.5 eV above the S_0 equilibrium structure. The analysis of the ^1L_a state along the PT coordinate reveals a gradual increase in the charge transfer character. No CI with other electronic states have been found along the reaction path.[34] Once on the S_0 surface, the excess vibrational energy from QM **6** is efficiently removed by back PT in accordance with the measured lifetime of QM **7** in CH_3CN of only 20 ns (see above).

The electronic character of the first two states of **S6·W** is analogous to **S6**. Upon stretching of the O–H bond, the energy of the ^1L_a state gradually rises as the proton is transferred from the OH group to the H_2O molecule (Figure 3). The barrier for the PT to H_2O amounts to $\Delta E^{ad}=0.61$ eV and $\Delta E^{ad}=0.68$ eV at the RI-CC2/cc-pVDZ and RI-CC2/aug-cc-pVDZ levels, respectively. In both cases this is comparable to the nuclear kinetic energy gain of the system at

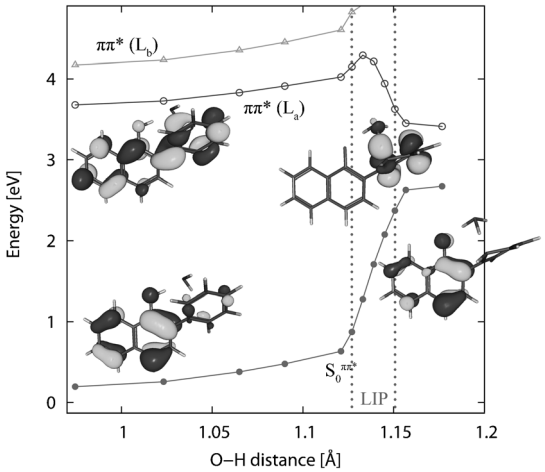

Figure 3. Minimum energy profiles of the ^1L_a state along the proton transfer coordinate in **S6·W**. The energies of the $S^{\pi\pi*}{}_0$ and ^1L_a have been calculated at the partially optimized ^1L_a geometries. In the region around the reaction barrier single point calculations along the linearly interpolated path (LIP) are performed to preserve the orientation of the system.[43]

the ^1L_a minimum, that is, the difference in energy between the vertical and the adiabatic excitations of 0.77 eV (RI-CC2/cc-pVDZ) and 0.58 eV (RI-CC2/aug-cc-pVDZ). The subsequent PT to the *ortho*-position of the phenyl ring is barrierless and leads to a CI with the S_0. However, at around at $R_{OH}=1.2$ Å the potential energy surface is very flat, with an almost negligible gradient between the oxygen and transferring H-atom suggesting the presence of a long-living species. This is in accordance with the measured lifetime of QM **7** in CH_3CN/H_2O, as well as with the observed increase of the QM **7** lifetime in CH_3CN/D_2O (3:1; see above). Moreover, since the H_2O-mediated ESPT pathway requires a localization of vibrational energy in the high fre-

quency O–H stretching mode, it is expected to occur on a longer time scale, and take place with lower quantum yield than direct ESIPT. The finding is consistent with the experimental observation of more efficient D-exchange at lower D_2O concentration.

De-excitation from S_1 provides the vibrational energy the system requires to overcome the **S6** *syn* to *anti* isomerization barrier of 4.54 kcal mol^{-1} (0.2 eV), leading to the higher population of **A6·W**. The electronic excitation of **A6·W** opens up new pathways; formation of naphtholate and solvent-mediated PT to the distal naphthalene positions 5, 7, and 8. In contrast to **S6·W**, the H_2O-mediated PT to the H_2O-bulk and to the naphthalene position 8 in **A6·W** is a barrierless reaction (Figure 4). In the first step, the naphthol OH proton is transferred to the H_2O molecule. The subsequent PT to the naphthalene position 8 delivers zwitterion **9**. The PT to the naphthalene position 8 corresponds to the lowest

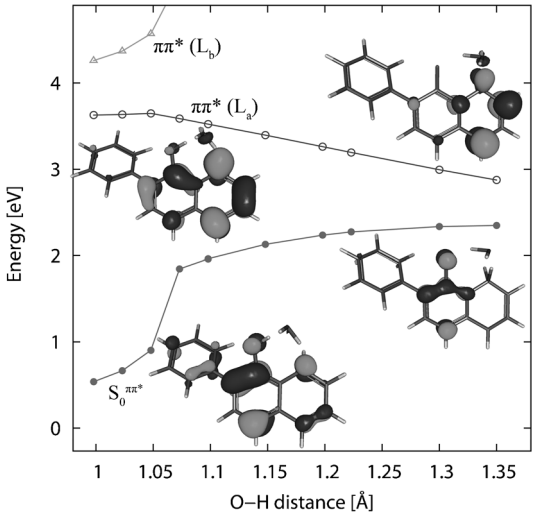

Figure 4. Minimum energy profiles of the ^1L_a state along the proton transfer coordinate in **A6·W**. The energies of the $S^{\pi\pi*}{}_0$ and ^1L_a, states have been calculated at the partially optimized geometries of ^1L_a. Occupied (bottom) and unoccupied (top) molecular orbitals of the ^1L_a state at the minimum energy geometry (left) and at $R_{OH}=1.35$ Å (right).

energy pathway, while PT to the positions 5 and 7 is favored by the largest negative charge on these atoms (See Table S11 in the Supporting Information).

Why is the quantum efficiency for ESIPT in **6** much higher than in any other investigated system?[13–19] For example in **3**, the optimization of the S_1 state of **S3**, leads directly to CI with S_0 as there is no minimum on the S_1 surface. However, the minimum energy structure of **3·W** is *anti* (see the Supporting Information). The energy difference of 1.46 kcal mol^{-1} between **A3·W** and **S3·W** corresponds to a Boltzmann population of the *syn* conformer of approximately 7% which is close to the observed Φ of D-incorporation in **3** ($\Phi=0.041$). This is an example of the operation of the NEER principle (nonequilibration of the excited-state rotamers) in control of the photochemical reactivity.[35]

Conclusion

In nonprotic solvents, **6** undergoes efficient ultrafast barrierless ESIPT along the surface of the ^1L_a state, delivering QM **7** via a CI with the S_0. Increase of H_2O concentration leads to an overall decrease in the quantum yield of ESIPT to the *ortho*-position of the adjacent phenyl. At the same time H_2O-cluster formation promotes PT to the distal naphthalene positions. The present photochemical and theoretical investigation has delineated the requirements for ESIPT to carbon to be an efficient process and thus opens the way to develop new examples and potential new applications of photochemical QM generation in biological and chemical systems.

Experimental Section

General: ^1H and ^{13}C NMR spectra were recorded on the machines operating at 300, 500, or 600 MHz. The NMR spectra were taken in $CDCl_3$ or [D_6]acetone at RT using TMS as a reference and chemical shifts were reported in ppm. For the assignation of the signals 2D homonuclear COSY and NOESY, and heteronuclear HSQC and HMBC correlation techniques were applied. UV/Vis spectra were recorded at rt. For the sample analysis the HPLC equipped with a Diode-Array detector and a C18 column was used. Mobile phase was CH_3OH/H_2O (15%). For the chromatographic separations silica gel (0.05–0.2 mm) was used. Analytical thin layer chromatography was performed on silica gel plates. MS were recorded on a HPLC-MS system using negative mode electrospray ionization technique. The deprotonation was achieved by use of triethylamine. Irradiation experiments were performed in reactors equipped with 2, 8 or, 16 lamps with the output at 254 nm or 300 nm. Chemicals (1-naphthol, triphenylbismuth and butyl lithium) were purchased from the usual commercial sources and were used as received. Solvents were purified by distillation.

Irradiation in CH_3CN/D_2O: To a solution of 2-phenyl-1-naphthol (**6**, 5 mg, 0.023 mmol) in CH_3CN (38 mL) was added D_2O (12 mL). The solution was purged with Ar for 30 min and irradiated in a Rayonet reactor at 254 or 300 nm (16 lamps) for 1 or 10 min. During irradiation, solution was continuously purged with Ar and cooled by a cold-finger condenser. After irradiation, 50 mL of H_2O was added and extractions with CH_2Cl_2 (3×50 mL) were carried out. The extracts were dried over anhydrous $MgSO_4$. After filtration and evaporation of the solvent, crude mixture was analyzed by NMR and MS.

Alternatively, 2-phenyl-1-naphthol (**6**, 10 mg, 0.046 mmol) was dissolved in CH_3CN (10 mL). The solution was divided into two parts and poured into two quartz cuvettes. To the first cuvette CH_3CN (10 mL) and D_2O (100 μL) were added, and to the second CH_3CN (5 mL) and D_2O (5 mL). Both solutions were purged with Ar (30 min), sealed and irradiated at the same time in a Luzchem reactor equipped with a merry-go-round using 8 lamps with the output at 300 nm for 1 h. To the irradiated solutions H_2O (20 mL) was added and extractions with CH_2Cl_2 (3×30 mL) were carried out. The extracts were dried over anhydrous $MgSO_4$. After filtration and evaporation of the solvent, crude mixture was analyzed by NMR and MS.

Control experiments were performed by preparing the same solution as described above that were kept in dark and worked-up with H_2O. After extractions with CH_2Cl_2 drying over anhydrous $MgSO_4$, filtration and evaporation of the solvent, the mixture was analyzed by NMR and MS.

Quantum yields for the D-incorporation: Solutions of **6** in CH_3CN/D_2O (3:1), as well as a solution of valerophenone in CH_3CN/H_2O (1:1) were freshly prepared and their concentrations adjusted to have absorbances 0.4–0.8 at 254 nm. After adjustment of the concentration and measurement of the corresponding UV/Vis spectra the solutions were filled in

quartz cuvettes (15 mL), purged with a stream of N_2 (20 min each), and sealed with a septum. The cuvettes were irradiated at the same time in a Luzchem reactor equipped with a merry-go-round and 2 lamps with the output at 254 nm for 0.5, 1, and 2 min. After each irradiation, the samples were taken from the cuvettes by use of a syringe and analyzed by ESI MS (the D content was determined from the difference of the intensity of signals of irradiated and nonirradiated sample), whereas the conversion of valerophenone was analyzed by HPLC. Quantum yields for the D-exchange was calculated using valerophenone actinometer (formation of acetophenone in aqueous media, $\Phi = 0.65 \pm 0.03$).[29]

Alternatively, 2-phenyl-1-naphthol (**1**, 5 mg, 0.023 mmol) was dissolved in CH_3CN (32 mL). To the solution was added D_2O (12 mL). The solution was purged with Ar for 30 min and irradiated in a Rayonet reactor at 254 (16 lamps) for 1 min. During irradiation, solution was continuously purged with Ar and cooled by a cold-finger condenser. After irradiation, 50 mL of H_2O was added and extractions with CH_2Cl_2 (3×50 mL) were carried out. The extracts were dried over anhydrous $MgSO_4$. Under the same conditions 2-phenylphenol (**2**, 6 mg, 0.03 mmol), dissolved in CH_3CN/D_2O (3:1, 50 mL) was irradiated for 10 min. After aqueous workup, extraction and removal of the solvent extent of the deuterium incorporation was determined by ^1H NMR. Quantum yield for the D-exchange was calculated using D-exchange in 2-phenylphenol as a secondary actinometer ($\Phi = 0.041 \pm 0.03$).[15]

Steady state and time-resolved fluorescence measurements: The steady state measurements were performed on a luminescence spectrometer. The samples were dissolved in cyclohexane, CH_3CN, or CH_3CN/H_2O (1:4) and the concentrations were adjusted to have absorbance at the excitation wavelength (300, 310, and 320 nm) < 0.1. Solutions were purged with nitrogen for 30 min prior to analysis. The measurements were performed at 20 °C. Fluorescence quantum yields were determined by comparison of the integral of the emission bands with the one of quinine sulfate in 0.05 M H_2SO_4 ($\Phi_f = 0.54$).[36] Typically, three absorption traces were recorded (and averaged) and three fluorescence emission traces, exciting at three different wavelengths (300, 310, and 320 nm). Three quantum yields were calculated and the mean value reported.

Fluorescence decay histograms were obtained on an, equipped with a light emitting diode (excitation wavelength 310 nm), using time-correlated single photon counting technique in 1023 channels. Histograms of the instrument response functions (using LUDOX scatterer), and sample decays were recorded until they reached 3×10^3 counts in the peak channel. The half width of the instrument response function was typically around 1.5 ns. The time increment per channel was 0.02 or 0.049 ns. Obtained histograms were fitted as sums of exponential using Gaussian-weighted nonlinear least-squares fitting based on Marquardt–Levenberg minimization implemented in the software package of the instrument. The fitting parameters (decay times and pre-exponential factors) were determined by minimizing the reduced chi-square χ^2. Additional graphical method was used to judge the quality of the fit that included plots of surfaces ("carpets") of the weighted residuals vs. channel number.

Laser flash photolysis (LFP): All LFP studies were conducted at the University of Victoria LFP facility employing a YAG laser, with a pulse width of 10 ns and excitation wavelength 266 nm. Static cells (0.7 cm) were used and solutions were purged with nitrogen or oxygen for 20 min prior to measurements. Absorbances at 266 nm were approximately 0.4.

Computational methods: The ground state equilibrium geometries of 2-phenylphenol (**3**) and 2-phenyl-1-naphthol (**6**) and their 1:1 H_2O-clusters, **3**·W and **6**·W, have been determined with the second order Møller–Plesset (MP2) method and the triple-zeta valence plus polarization (TZVP) basis set.[37] Solvation effects were estimated with the polarizable continuum model (PCM)[38] using the dielectric constant of CH_3CN as implemented in the Gaussian09 program package.[39] The vertical excitation energies, optimized geometries, and ESIPT reaction paths have been determined with the second order approximate coupled cluster (CC2) method with the cc-pVDZ and aug-cc-pVDZ basis sets.[40] The resolution of identity (RI) approximation has been used for the evaluation of the electron repulsion integrals.[41] Two types of reaction path calculations have been employed. In the relaxed scans, apart from the driving coordinate all other internal degrees of freedom have been allowed to relax. In the region between the vertical and adiabatic geometries a set of single point calculations for geometries along the linearly interpolated path (LIP) have been performed. LIP geometries have been obtained by interpolating between terminal geometries in internal coordinates. All coupled cluster calculations have been performed with the TURBOMOLE package.[42]

Acknowledgements

This work was financed by the Foundation for Science, Higher Education and Technological Development of Croatia (HRZZ grant No. 02.05/25), the Ministry of Science Education and Sports of Croatia (grant No. 098–0352851–2921), the University of Victoria, and the Natural Sciences and Engineering Research Council (NSERC) of Canada.

[1] a) J. F. Ireland, P. A. H. Wyatt, *Adv. Phys. Org. Chem.* **1976**, *12*, 131–221; b) S. J. Formosinho, L. G. Arnaut, *J. Photochem. Photobiol. A: Chem.* **1993**, *75*, 21–48; c) S. M. Ormson, R. G. Brown, *Prog. React. Kinet.* **1994**, *19*, 45–91; d) D. Le Gourrierec, S. M. Ormson, R. G. Brown, *Prog. React. Kinet.* **1994**, *19*, 211–275; e) A. Sinicropi, R. Pogni, R. Basosi, M. A. Robb, G. Gramlich, W. M. Nau, M. Olivucci, *Angew. Chem. Int. Ed.* **2001**, *40*, 4185–4189.
[2] J. I. Kwon, S. Y. Park, *Advan. Mater.* **2011**, *23*, 3615–3642.
[3] a) K. Choi, A. D. Hamilton, *Angew. Chem. Int. Ed.* **2001**, *40*, 3912–3915; b) A. S. Klymchenko, A. P. Demchenko, *J. Am. Chem. Soc.* **2002**, *124*, 12372–12379; c) X. Peng, Y. Wu, J. Fan, M. Tian, K. Han, *J. Org. Chem.* **2005**, *70*, 10524–10531; d) R. M. F. Batista, E. Oliveira, S. P. G. Costa, C. Lodeiro, M. M. M. Raposo, *Org. Lett.* **2007**, *9*, 3201–3204.
[4] S. Arumugam, V. V. Popik, *J. Am. Chem. Soc.* **2011**, *133*, 5573–5579.
[5] a) D. A. Parthenopoulos, D. P. McMorrow, M. Kasha, *J. Phys. Chem.* **1991**, *95*, 2668–2674; b) A. Douhal, F. Amat-Guerri, A. U. Acuña, K. Yoshihara, *Chem. Phys. Lett.* **1994**, *217*, 619–625; c) S. Park, O.-H. Kwon, S. Kim, S. Park, M.-G. Choi, M. Cha, S. Y. Park, D.-J. Jang, *J. Am. Chem. Soc.* **2005**, *127*, 10070–10074.
[6] a) G. J. Stueber, M. Kieninger, H. Schettler, W. Busch, B. Goeller, J. Franke, H. E. A. Kramer, H. Hoier, S. Henkel, P. Fischer, H. Port, T. Hirsch, G. Rytz, J.-L. Birbaum, *J. Phys. Chem.* **1995**, *99*, 10097–10109; b) J. Keck, H. E. A. Kramer, H. Port, T. Hirsch, P. Fischer, G. Rytz, *J. Phys.Chem.* **1996**, *100*, 14468–14475.
[7] a) J. M. Kauffman, *Radiation Phys. Chem.* **1993**, *41*, 365–371; b) A. Pla-Dalmau, *J. Org. Chem.* **1995**, *60*, 5468–5473.
[8] L. V. Schäfer, G. Groenhof, A. R. Klingen, G. L. Ullmann, M. Boggio-Pasqua, M. A. Robb, H. Grubmüller, *Angew. Chem. Int. Ed.* **2007**, *46*, 530–536.
[9] R. M. D. Nunes, M. Pineiro, L. G. Arnaut, *J. Am. Chem. Soc.* **2009**, *131*, 9456–9462.
[10] T. Mutai, H. Tomoda, T. Ohkawa, Y. Yabe, K. Araki, *Angew. Chem. Int. Ed.* **2008**, *47*, 9522–9524.
[11] M. Kasha, *J. Chem. Soc. Faraday Trans. 2* **1986**, *82*, 2379–2392.
[12] a) N. Basarić, P. Wan, *Photochem. Photobiol. Sci.* **2006**, *5*, 656–664; b) N. Behin Aein, P. Wan, *J. Photochem. Photobiol. A: Chem.* **2009**, *208*, 42–49; c) N. Basarić, N. Cindro, Y. Hou, I. Žabčić, K. Mlinarić-Majerski, P. Wan, *Can. J. Chem.* **2011**, *89*, 221–234.
[13] S. P. Webb, L. A. Philips, S. W. Yeh, L. M. Tolbert, J. H. Clark, *J. Phys. Chem.* **1986**, *90*, 5154–5164.
[14] M. Lukeman, D. Veale, P. Wan, R. N. Munasinghe, J. E. T. Corrie, *Can. J. Chem.* **2004**, *82*, 240–253.
[15] a) M. Lukeman, P. Wan, *Chem. Commun.* **2001**, 1004–1005; b) M. Lukeman, P. Wan, *J. Am. Chem. Soc.* **2002**, *124*, 9458–9464.
[16] M. Lukeman, P. Wan, *J. Am. Chem. Soc.* **2003**, *125*, 1164–1165.
[17] a) M. Flegel, M. Lukeman, L. Huck, P. Wan, *J. Am. Chem. Soc.* **2004**, *126*, 7890–7897; b) N. Basarić, P. Wan, *J. Org. Chem.* **2006**, *71*, 2677–2686; c) L. Y.-H. Wang, P. Wan, *Photochem. Photobiol. Sci.* **2011**, *10*, 1934–1944.

[18] M. K. Nayak, P. Wan, *Photochem. Photobiol. Sci.* **2008**, *7*, 1544–1554.
[19] M. Lukeman, M.-D. Burns, P. Wan, *Can. J. Chem.* **2011**, *89*, 433–440.
[20] a) S. S. Lehrer, *J. Am. Chem. Soc.* **1970**, *92*, 3459–3462; b) H. Shizuka, M. Serizawa, H. Kobayashi, K. Kameta, H. Sugiyama, T. Matsuura, I. Saito, *J. Am. Chem. Soc.* **1988**, *110*, 1726–1732.
[21] Ed. S. E. Rokita, *Quinone Methides*, Wiley, New York, **2009**.
[22] T. P. Pathak, M. S. Sigman, *J. Org. Chem.* **2011**, *76*, 9210–9215.
[23] a) H. Kang, S. E. Rokita, *Nucl. Acid Res.* **1996**, *24*, 3896–3902; b) Q. Zhou, Q. S. E. Rokita, *Proc. Natl. Acad. Sci. U. S. A.* **2003**, *100*, 15452–15457; c) H. Wang, M. S. Wahi, S. E. Rokita, *Angew. Chem. Int. Ed.* **2008**, *47*, 1291–1293; d) H. Wang, S. E. Rokita, *Angew. Chem. Int. Ed.* **2010**, *49*, 5997–5960.
[24] a) S. E. Wolkenberg, D. L. Boger, *Chem. Rev.* **2002**, *102*, 2477–2495; b) P. Wang, Y. Song, L. Zhang, H. He, X. Zhou, *Curr. Med. Chem.* **2005**, *12*, 2893–2913.
[25] a) J. Wirz, *Pure Appl. Chem.* **1998**, *70*, 2221–2232; b) A. P. Pelliccioli, P. Šebej, J. Wirz, *Photochem. Photobiol. Sci.* **2012**, *11*, 967–971.
[26] a) D. H. R. Barton, J. C. Blazejewski, B. Charpiot, D. J. Lester, W. B. Motherwell, M. T. B. Papoula, *J. Chem.Soc. Chem. Commun.* **1980**, 827–829; b) D. H. R. Barton, N. Y. Bhatnagar, J. C. Blazejewski, B. Charpiot, J. P. Finet, D. J. Lester, W. B. Motherwell, M. T. B. Papoula, S. P. J. Stanforth, *Chem. Soc. Perkin Trans. 1* **1985**, 2657–2665.
[27] Y. Ahmad, D. H. Hey, *J. Chem. Soc.* **1959**, 3819–3822.
[28] H. Shizuka, S. Tobita, *J. Am. Chem. Soc.* **1982**, *104*, 6919–6921.
[29] H. J. Kuhn, S. E. Braslavsky, R. Schmidt, *Pure Appl. Chem.* **2004**, *76*, 2105–2146.
[30] a) M. Capponi, I. G. But, B. Hellrung, G. Persy, J. Wirz, *Can. J. Chem.* **1999**, *77*, 605–613; b) I. Glynne Gut, L. C. Scheibler, J. Wirz, *Photochem. Photobiol. Sci.* **2010**, *9*, 901–907.
[31] According to NMR spectra of the deuterated sample obtained on photolysis in CH_3CN/D_2O (3:1) relative ratio of **7**/**8**/**9** is estimated to be 10:1.3:1. Formation of **10**–**12** may also be possible in an overall quantum yield similar to that of **8**. Due to the overlapping signals of the naphthalene H-atoms at the positions 4, 6, and 7 their relative ratio cannot be given.
[32] a) F. G. Bordwell, J.-P. Cheng, *J. Am. Chem. Soc.* **1991**, *113*, 1736–1743; b) H. Mohan, R. Hermann, S. Naumov, J. P. Mittal, O. Brede, *J. Phys. Chem. A* **1998**, *102*, 5754–5762; c) D. Shukla, N. P. Schepp, N. Mathivanan, L. J. Johnston, *Can. J. Chem.* **1997**, *75*, 1820–1829; d) T. A. Gadosy, D. Shukla, L. J. Johnston, *J. Phys. Chem. A* **1999**, *103*, 8834–8839.
[33] E. Pines, in *The Chemistry of Phenols*, (Ed.: Z. Rappoport), Wiley, New York, **2003**.
[34] a) A. L. Sobolewski, W. Domcke, *J. Phys. Chem. A* **2001**, *105*, 9275–9283; b) Z. Lan, W. Domcke, V. Vallet, A. L. Sobolewski, S. Mahapatra, *J. Chem. Phys* **2005**, *122*, 224315–224313; c) A. L. Sobolewski, W. Domcke, *J. Phys Chem. A* **2007**, *111*, 11725–11735.
[35] a) H. J. Jacobs, E. Havinga, *Adv. Photochem.* **1979**, *11*, 305–373; b) U. Mazzucato, F. Momicchioli, *Chem. Rev.* **1991**, *91*, 1679–1719.
[36] W. R. Dawson, M. W. Windsor, *J. Phys. Chem.* **1968**, *72*, 3251–3260.
[37] K. Eichkorn, O. Treutler, H. Öhm, M. Häser, R. Ahlrichs, *Chem. Phys. Lett.* **1995**, *242*, 652–660.
[38] J. Tomasi, B. Mennucci, R. Cammi, *Chem. Rev.* **2005**, *105*, 2999–3094.
[39] Gaussian 09, Revision A.02, M. J. Frisch, G. W. Trucks, H. B. Schlegel, G. E. Scuseria, M. A. Robb, J. R. Cheeseman, G. Scalmani, V. Barone, B. Mennucci, G. A. Petersson, H. Nakatsuji, M. Caricato, X. Li, H. P. Hratchian, A. F. Izmaylov, J. Bloino, G. Zheng, J. L. Sonnenberg, M. Hada, M. Ehara, K. Toyota, R. Fukuda, J. Hasegawa, M. Ishida, T. Nakajima, Y. Honda, O. Kitao, H. Nakai, T. Vreven, J. A. Montgomery, Jr., J. E. Peralta, F. Ogliaro, M. Bearpark, J. J. Heyd, E. Brothers, K. N. Kudin, V. N. Staroverov, R. Kobayashi, J. Normand, K. Raghavachari, A. Rendell, J. C. Burant, S. S. Iyengar, J. Tomasi, M. Cossi, N. Rega, J. M. Millam, M. Klene, J. E. Knox, J. B. Cross, V. Bakken, C. Adamo, J. Jaramillo, R. Gomperts, R. E. Stratmann, O. Yazyev, A. J. Austin, R. Cammi, C. Pomelli, J. W. Ochterski, R. L. Martin, K. Morokuma, V. G. Zakrzewski, G. A. Voth, P. Salvador, J. J. Dannenberg, S. Dapprich, A. D. Daniels, Ö. Farkas, J. B. Foresman, J. V. Ortiz, J. Cioslowski, and D. J. Fox, Gaussian, Wallingford CT, 2009.
[40] O. Christiansen, H. Koch, P. Jorgensen, *Chem. Phys. Lett.* **1995**, *243*, 409–418.
[41] F. Weigend, M. Häser, *Theor. Chem. Acc.* **1997**, *97*, 331–340.
[42] R. Ahlrichs, M. Bär, M. Häser, H. Horn, C. Kölmel, *Chem. Phys. Lett.* **1989**, *162*, 165–169.
[43] B. Auer, L. E. Fernandez, S. Hammes-Schiffer, *J. Am. Chem. Soc.* **2011**, *133*, 8282–8292.

Received: April 4, 2012
Published online: July 10, 2012

